Nematic state stabilized by off-site Coulomb interaction in iron-based superconductors

Xiao-Jun Zheng,[1] Zhong-Bing Huang,[2,3,*] Da-Yong Liu,[1] and Liang-Jian Zou[1,4,†]

[1]*Key Laboratory of Materials Physics, Institute of Solid State Physics, Chinese Academy of Sciences, P. O. Box 1129, Hefei 230031, China*

[2]*Faculty of Physics and Electronic Technology, Hubei University, Wuhan 430062, China*

[3]*Beijing Computational Science Research Center, Beijing 100084, China*

[4]*Department of Physics, University of Science and Technology of China, Hefei 230026, China*

(Received 28 March 2014; revised manuscript received 23 July 2015; published 6 August 2015)

Using a variational Monte Carlo method, we investigate the nematic state in iron-based superconductors based on the three-band Hubbard model. Our results demonstrate that the nematic state, formed by introducing an anisotropic hopping order into the projected wave function, can arise in the underdoped regime by an off-site Coulomb interaction V induced d-wave Pomeranchuk instability. An analysis of V in momentum space indicates that the interaction between electrons around $(\pi,0)$ and $(0,\pi)$ points is crucial for the formation of the nematic state. The resulting anisotropic kinetic energy and spin correlation, as well as unequal occupation of d_{xz} and d_{yz} orbitals, are all suppressed upon electron doping, which are consistent with the doping dependence of intrinsic anisotropy revealed by optical spectrum measurement and angle-resolved photoemission spectroscopy.

DOI: 10.1103/PhysRevB.92.085109 PACS number(s): 71.10.Fd, 74.25.Jb, 74.70.Xa

I. INTRODUCTION

Recently the electronic nematic phase, in which the discrete lattice rotational symmetry is broken but the translational symmetry is retained [1,2], has been observed and widely discussed in correlated electron systems, such as bilayer Ruthenate [3], high-T_c cuprates [4–10], and iron-based superconductors (FeSCs) [11–20]. Since its possible relation to the high-T_c superconductivity, this phenomenon in the later two systems has highly attached importance and received considerable attention.

In high-T_c cuprates, the nematic state is induced either by a d-wave Pomeranchuk instability [21–25] or via quantum melting of charge stripes [1,26]. As for FeSCs, the situation can be quite different. First, in contrast to the Mott insulator in cuprates, the parent phase of FeSCs is metallic, suggesting that the conduction electrons in FeSCs are less correlated. Second, in most of FeSCs, the ordering vector of the long-range magnetic order is $(\pi, 0)$ or $(0, \pi)$ [27–29], which is different from the (π, π) ordering vector in high-T_c cuprates. This stripelike antiferromagnetic (SAFM) state which occurs at T_N is always preceded by or coincident with a tetragonal-to-orthorhombic structural transition at T_S (see Ref. [30] for review). Both of these two transitions break the fourfold rotational symmetry down to a twofold symmetry. Furthermore, it is widely believed that high-T_c cuprates could be described by a single-band model, distinct from the multiband electronic structure of FeSCs.

The nematic phase in FeSCs is manifested by the onset of anisotropies of dc resistivity [11], optical conductivity [31,32], and orbital polarization of d_{yz} and d_{xz} Fe states [12,18] above T_S in the tetragonal structure. These anisotropies in experiments are much stronger than those from the slight difference of lattice constants driven by the structural transition. For this reason, many theorists consider that the nematic states are electronic correlation driven, and two scenarios are proposed: One scenario considers magnetic fluctuations as the driving force of the nematic state [15–17,33]; the other one [14,34,35] takes the orbital ordering as the driving force, i.e., the degeneracy between $3d$ xz and yz orbitals is spontaneously broken, and the resulting orbital occupation renormalizes the exchange constants and triggers the magnetic transition at a lower temperature. Currently it remains unclear how to distinguish these two phenomenological scenarios due to the coupling between spin and orbital degrees of freedom.

While quite a number of experimental phenomena have been explained by either of these two scenarios, some important issues need to be clarified. One of them is that although electronic correlations are taken as the driving force of the nematic state, most of the analysis was based on phenomenological models, and no solid analysis based on realistic models has been done so far. As electronic correlations in FeSCs are weaker than in high-T_c cuprates, whether they can play the same role as the one in high-T_c cuprates is under doubt. Another important issue is the doping dependence of the nematic state. While experiments of dc resistivity in the Co doping compounds show that the anisotropy of dc resistivity develops with increasing concentration of dopant atoms [36–39], optical spectrum measurement [36] and angle-resolved photoemission spectroscopy (ARPES) [12] found that the anisotropy of optical conductivity and energy splitting of bands with dominant xz and yz characters behave in the opposite way. These phenomena make people reconsider the roles of intrinsic and extrinsic anisotropies playing in the dc anisotropy.

To gain a further insight into the nematic state in FeSCs, especially for its microscopic origin, we perform a variational Monte Carlo study on a three-band (3B) Hubbard model with large lattice sizes ranging from 20×20 to 24×24. A highlight of our model is that an off-site Coulomb interaction V is included, which is neglected so far, to our knowledge, in all the analysis of FeSCs, but played an important role in the formation of nematic order in $Sr_3Ru_2O_7$ [40] and high-T_c cuprates [7,10,23,25]. The numerical results presented below (see Figs. 1 and 3) indicate that similar to high-T_c cuprates, V is crucial for stabilizing the nematic state in

*huangzb@hubu.edu.cn

†zou@theory.issp.ac.cn

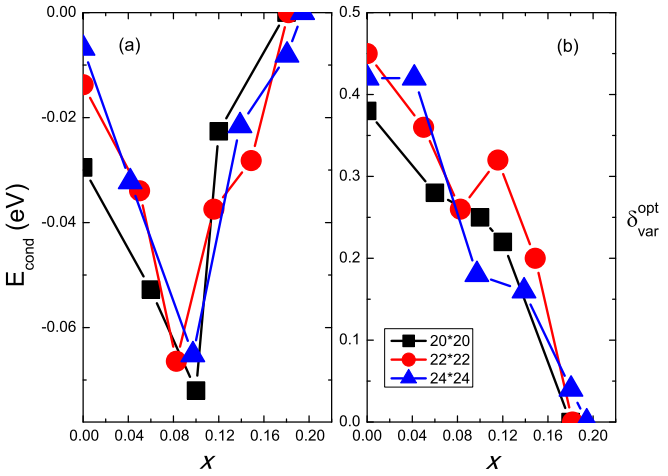

FIG. 1. (Color online) Condensation energy $E_{\rm cond}$ (a) and optimized value of $\delta_{\rm var}$ (b) as a function of electron doping on the 20×20, 22×22, and 24×24 lattices.

FeSCs. Our variational calculations also confirm that the intrinsic anisotropy in the nematic state is suppressed upon electron doping, just as the one observed by optical spectrum measurement and ARPES experiments.

Our paper is organized as follows: In Sec. II we define the Hamiltonian and describe the variational Monte Carlo method. In Sec. III we present our numerical results and discuss their relation to the experimental measurements. Finally, we make some concluding remarks in Sec. IV.

II. MODEL AND NUMERICAL APPROACH

The two-dimensional 3B Hubbard model is given as

$$\begin{aligned} H = H_0 + U_1 \sum_{i\alpha} n_{i\alpha\uparrow} n_{i\alpha\downarrow} + \sum_{i,\alpha<\beta,\sigma,\sigma'} [(U_2 - J\delta_{\sigma\sigma'}) n_{i\alpha\sigma} n_{i\beta\sigma'}] \\ + J \sum_{i,\alpha<\beta} (c^\dagger_{i\alpha\uparrow} c^\dagger_{i\beta\downarrow} c_{i\alpha\downarrow} c_{i\beta\uparrow} + c^\dagger_{i\alpha\uparrow} c^\dagger_{i\alpha\downarrow} c_{i\beta\downarrow} c_{i\beta\uparrow} + \text{H.c.}) \\ + V \sum_{\langle ij \rangle} n_i n_j, \end{aligned} \tag{1}$$

here H_0 is the kinetic part of the Hamiltonian, with transfer parameters $t^0_{\alpha\beta}[\Delta x, \Delta y]$ taken from Ref. [41]. We define N as the number of sites and n the average number of electrons per site. For the undoped case, $n = 4$. The doping level x is then defined as $x = n - 4$. The interaction part of the model includes intraorbital and interorbital Coulomb interaction U_1, U_2, the Hund coupling J, as well as the Coulomb interaction V between nearest-neighbor (NN) sites.

The wave function we use is as the following:

$$|\psi\rangle = P_G |\psi_{\rm MF}\rangle = g_1^{\hat{N}_1} g_2^{\hat{N}_2} g_V^{\hat{N}_V} g_J^{\hat{N}_J} |\psi_{\rm MF}\rangle, \tag{2}$$

where

$$\begin{aligned} \hat{N}_1 &= \sum_{i,\alpha} n_{i\alpha\uparrow} n_{i\alpha\downarrow}, \quad \hat{N}_2 = \sum_{i,\alpha<\beta} n_{i\alpha} n_{i\beta}, \\ \hat{N}_V &= \sum_{\langle ij \rangle} n_i n_j, \quad \hat{N}_J = \sum_{i,\alpha<\beta,\sigma} n_{i\alpha\sigma} n_{i\beta\sigma}, \end{aligned} \tag{3}$$

g_1, g_2, g_J are the variational parameters controlling the number of electrons residing in the same and different on-site orbitals. g_V controls the number of electrons on the NN sites.

To investigate the nematic state, an anisotropic hopping order (AHO) with order parameter $\delta_{\rm var}$ is introduced. This kind of introducing nematic order has successfully captured the nature of the nematic state in high-T_c cuprates [8,10]. A noninteracting variational Hamiltonian $H_{\rm MF}$ is then obtained by substituting some of hopping parameter $t^0_{\alpha\beta}[\Delta x, \Delta y]$ in H_0 by

$$\begin{aligned} t^{\rm MF}_{\alpha\beta}[\Delta x, 0] &= (1 + \delta_{var}) t^0_{\alpha\beta}[\Delta x, 0], \\ t^{\rm MF}_{\alpha\beta}[0, \Delta y] &= (1 - \delta_{var}) t^0_{\alpha\beta}[0, \Delta y]. \end{aligned} \tag{4}$$

The wave function $|\psi_{\rm MF}\rangle$ is then obtained by diagonalizing the quadratic Hamiltonian $H_{\rm MF}$. In this paper we will focus on the nematic state in the high temperature paramagnetic regime and take AHO as the only order parameter. Some limited calculations (not shown) show that the striped antiferromagnetic state has a lower energy than the nematic state, indicating that the ground state of FeSCs lies in a magnetic state, which is consistent with experimental measurements.

Unless otherwise stated, the values of the interacting parameters are $U_1 = 2.0$, $U_2 = 1.0$, $J = 0.5$, and $V = 0.5$ in units of eV in this paper, which correspond to typical values of iron-based superconductors. According to the *ab initio* calculations [42], we consider that setting $V = 0.5$ is also appropriate.

Our calculations are performed for square lattices with periodic boundary conditions along the x and y directions. The ground state energy $\langle \psi | H | \psi \rangle$ is calculated using a standard Markovian chain Monte Carlo approach with a Metropolis update algorithm, and is optimized with respect to the variational parameters. During the optimization, a quasi-Newton method combined with the fixed sampling method [43,44] is used. In the figures presented below, the statistical errors are smaller than the symbol size unless otherwise stated.

III. RESULTS AND DISCUSSIONS

The condensation energy per unit cell $E_{\rm cond}$ $\{= [E(\delta^{\rm opt}_{\rm var}) - E(0)]/N$, with $\delta^{\rm opt}_{\rm var}$ being the optimized AHO parameter$\}$ as a function of doping is presented in Fig. 1(a). The results on the 20×20, 22×22, and 24×24 lattices consistently show that $|E_{\rm cond}|$ exhibits a nonmonotonic doping dependence, with a maximum at finite doping around $x = 0.08$–0.10, and vanishes when x is larger than 0.18. This behavior is quite different from that in high-T_c cuprates, where a monotonic decrease of the condensation energy with increasing the doping density was observed [8,10]. The condensation energies, with the largest value around 70 meV, provide a strong evidence that the nematic state in FeSCs can be driven purely by electronic correlations. The doping dependence of $\delta^{\rm opt}_{\rm var}$ is shown in Fig. 1(b). One can see that $\delta^{\rm opt}_{\rm var}$ has a maximum value in the undoped case, and then is suppressed by increasing the electron doping.

In Fig. 1 one can notice that although the curves corresponding to different lattices basically exhibit the same trend, they are seen to be size dependent and show a nonmonotonic behavior at some doping levels. This is induced by the finite

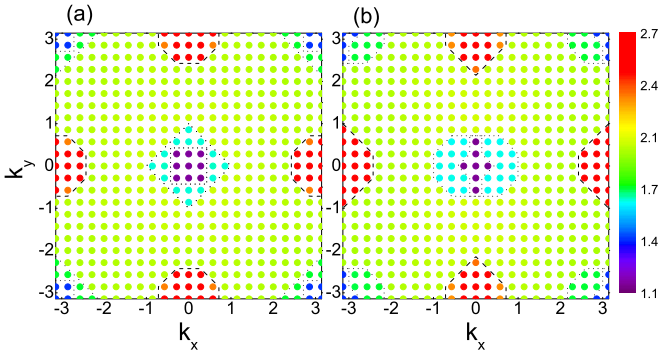

FIG. 2. (Color online) Electron occupation $n(k)$ in the normal state ($\delta_{\rm var} = 0.0$) (a) and in the nematic state ($\delta_{\rm var} = 0.5$) (b) on the 22×22 lattice at $x = 0$. The dashed and dotted lines, across which distinct colors manifest a finite change of $n(k)$, denote the electron and hole Fermi pockets, respectively.

size effect [8,10], which is manifested in our study by a discontinuous change of Fermi surfaces (FSs) consisted of discrete k points when the value of the variational parameter $\delta_{\rm var}$ changes. As as result, uncertainty (estimated about 0.05–0.08) is raised to $\delta_{\rm var}^{\rm opt}$, which then brings uncertainties to $E_{\rm cond}$ and other physical quantities shown in Fig. 5. However, the universal behaviors and quantitatively agreement results within uncertainties on different lattices demonstrate that our findings reflect the intrinsic properties of the studied model.

With the development of nematic order, the FSs spontaneously break their fourfold symmetry. As shown in the left panel of Fig. 2, the FSs at $x = 0$ in the normal state are highly symmetric. In the nematic state, one of the main consequences is that all of the FSs become twofold symmetric, as seen in the right panel of Fig. 2. The electron Fermi pockets around $k = (\pm\pi,0)$ points expand considerably along the y direction, whereas the electron Fermi pockets around $k = (0, \pm\pi)$ points tend to shrink along the x direction; The hole FSs around $k = (0,0)$ and $k = (\pi,\pi)$ points display similar changes, and the rotational symmetry is reduced to a twofold one. This kind of FS distortion was also observed in high-T_c cuprates [10,22–24].

In order to identify the physical origin for the formation of the nematic phase, in Fig. 3(a) we present different energy contributions $\Delta E_\alpha = [E_\alpha(\delta_{\rm var}^{\rm opt}) - E_\alpha(0)]/N$ as a function of electron doping on the 20×20 lattice, with α representing different components of the Hamiltonian. In contrast to the positive contributions from the kinetic and on-site U parts, a pronounced gain of Coulomb potential energy from the V part demonstrates that the off-site Coulomb interaction V plays a crucial role in stabilizing the nematic state. Figure 3(b) shows that with decreasing V, $E_{\rm cond}$ is reduced dramatically and vanishes for $V \leqslant 0.35$. Considering that Coulomb screening effect will reduce the magnitude of V as the electron doping is increased, it is expected that both $|E_{\rm cond}|$ and $\delta_{\rm var}^{\rm opt}$ in the realistic electron-doped system should be smaller than those presented in Fig. 1 with a fixed V. For this reason, the extent of the doping regime in which the nematic phase exists will shrink if a more realistic V is used, making our results more comparable with the experiments, where the nematic characters were observed only in a narrow underdoped regime.

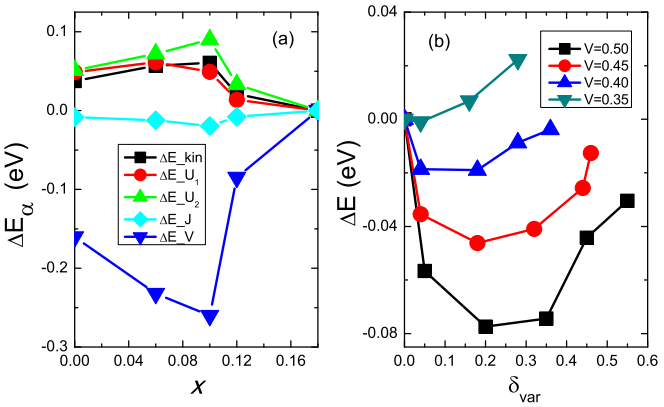

FIG. 3. (Color online) (a) Different energy contributions to the condensation energy as a function of electron doping on the 20×20 lattice. (b) Total energy change as a function of $\delta_{\rm var}$ for different values of V on the 20×20 lattice at $x = 0.10$. The different parts of Hamiltonian and the value of V are indicated by the shape of the symbol in (a) and (b), respectively.

The role of V in stabilizing the nematic state could also be seen clearly from the expression of mean-field decoupled exchange part of V in momentum space [25], which has the form of

$$V(\mathbf{k}) = -2V \sum_{\mathbf{k}'} [\cos(k_x - k'_x) + \cos(k_y - k'_y)] n(\mathbf{k}'). \tag{5}$$

Here $n(k)$ is the occupation of k in momentum space. In terms of Eq. (5), one finds that the interaction between electrons around $(\pi,0)$ and $(0,\pi)$ points in the Brillouin zone is positive, while the one between electrons around $(\pi,0)$ and $(-\pi,0)$ points is negative, as clearly shown in Fig. 4. This interaction is very similar to the effective d-wave interaction introduced in the phenomenological forward scattering model [22,24]. According to the forward scattering

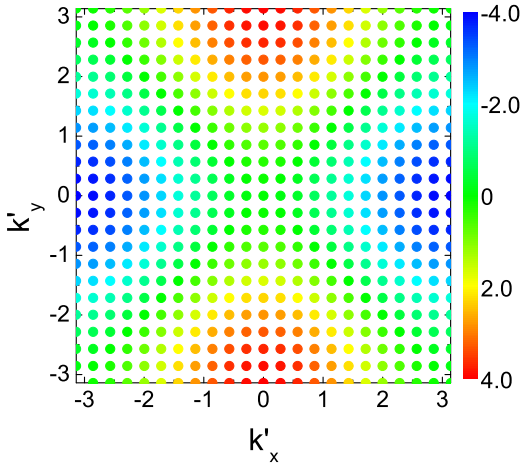

FIG. 4. (Color online) Momentum ($\mathbf{k}'$) dependence of the interaction $-2[\cos(k_x - k'_x) + \cos(k_y - k'_y)]$ on the 22×22 lattice at $\mathbf{k} = (\pi,0)$. Notice that the interaction occurs mainly for electrons around the borders of the Brillouin zone and exhibits a twofold symmetry.

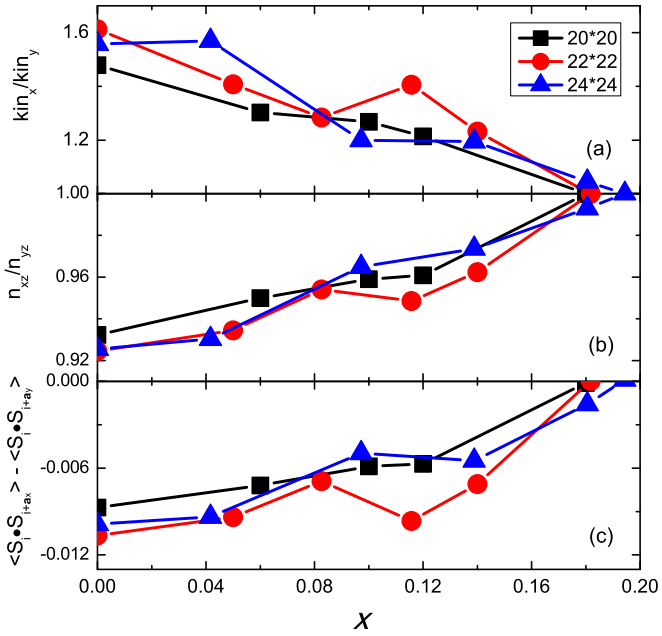

FIG. 5. (Color online) Ratio of kin_x and kin_y (a), n_{xz}/n_{yz} (b), and $\langle S_i \cdot S_{i+\mathbf{a}_x}\rangle - \langle S_i \cdot S_{i+\mathbf{a}_y}\rangle$ (c) as a function of electron doping on the 20×20, 22×22, and 24×24 lattices. The kinetic energies kin_x and kin_y are defined in the text.

model, the effective d-wave interaction, namely the attractive interaction between electrons on opposite corners of the Fermi surface and the repulsive interaction between electrons on neighboring corners, is the driving force for the nematic instability. Therefore, it is expected that the off-site Coulomb interaction is helpful for the formation of the nematic phase in iron pnictides.

The results displayed in Figs. 3 and 4 indicate that a substantial V and the existence of electron Fermi pockets around $(\pi,0)$ and $(0,\pi)$ are necessary conditions for the formation of the nematic state in FeSCs. This is in contrast to the magnetic or orbital scenario based on an itinerant electron picture [16,17], where the interpocket interaction U_{eff} between hole pockets around $(0,0)$ and electron pockets around $(\pi,0)$ and $(0,\pi)$ is crucial for enhancing magnetic or orbital fluctuations with wave vectors $\mathbf{Q_X}=(\pi,\mathbf{0})$ and $\mathbf{Q_Y}=(\mathbf{0},\pi)$, which then drive FeSCs to the nematic state. Since the V induced interaction is vanishingly small between hole and electron pockets (see Fig. 4), it is hard to understand our findings in terms of the magnetic or orbital scenario. Moreover, NN spin correlation, i.e., $\langle S_i \cdot S_{i+\mathbf{a}_{x/y}}\rangle$ with $\mathbf{a}_{x/y}$ denoting the unit vector along the x/y direction, was found to be dramatically suppressed in the regime $V > 0.35$. Thus, the magnetic scenario seems to be inapplicable in the case that V makes a dominant contribution to the stabilization of the nematic state.

As the doping dependence of the nematic state is an important issue, now we turn to discuss the doping-dependent properties of our results and their relations to the experimental measurements. Figures 5(a) and 5(b) show the ratios of kinetic energies along the x and y directions and of electron occupations in the d_{xz} and d_{yz} orbitals, which are defined as $\mathrm{kin}_x/\mathrm{kin}_y = \langle\sum_{i\alpha\beta\sigma\Delta x} t^0_{\alpha\beta}[\Delta x,0]c^\dagger_{i,\alpha\sigma}c_{i+\Delta x,\beta\sigma}\rangle/\langle\sum_{i\alpha\beta\sigma\Delta y} t^0_{\alpha\beta}[0,\Delta y]c^\dagger_{i,\alpha\sigma}c_{i+\Delta y,\beta\sigma}\rangle$ and n_{xz}/n_{yz}, respectively. Figure 5(c) displays the difference between spin correlations along the x and y directions, defined as $\langle S_i \cdot S_{i+\mathbf{a}_x}\rangle - \langle S_i \cdot S_{i+\mathbf{a}_y}\rangle$. We can see that anisotropies are introduced in the kinetic energy, electron occupation, and magnetic correlation by AHO, and exhibit the same doping dependence as $\delta^{\mathrm{opt}}_{\mathrm{var}}$. These simultaneous anisotropies can be naturally explained by the V induced d-wave Pomeranchuk instability. On the one hand, the Fermi surface deformations shown in Fig. 2 lead to a lifting of two degenerate magnetic channels with wave vectors $\mathbf{Q_X}=(\pi,\mathbf{0})$ and $\mathbf{Q_Y}=(\mathbf{0},\pi)$. On the other hand, the orbital order is produced since the electron pockets centered at $(\pi,0)$ and $(0,\pi)$ have different orbital characters. Due to the hybridization of d_{xz}, d_{yz}, and d_{xy} bands near $(\pi,0)$ and $(0,\pi)$, the Fermi surface deformations also result in a band reconstruction for all bands in the nematic state, as observed in recent ARPES experiment [45].

The decrease of anisotropy of orbital occupation with increasing the doping density is consistent with the behavior of energy splitting of bands with dominant xz and yz characters observed by ARPES [12]. According to the standard linear-response theory [46,47], the optical conductivity and Drude weight could be expressed as

$$\tilde{\sigma}_{x/y}(\omega) = -\frac{\langle\hat{T}_{x/y}\rangle}{i\omega} - \frac{1}{i\omega}\sum_{m\neq 0}\frac{|\langle m|\hat{J}_{x/y}|0\rangle|^2}{\omega-(E_m-E_0)+i0^+},$$

$$D_{x/y} = -\pi\langle\hat{T}_{x/y}\rangle - 2\pi\sum_{m\neq 0}\frac{|\langle m|\hat{J}_{x/y}|0\rangle|^2}{E_m-E_0}. \tag{6}$$

Here $|0\rangle$ and $|m\rangle$ represent the ground state and the mth excited state. The T operators are derived as

$$\hat{T}_x = \sum_{i,\Delta x,\Delta y,\alpha,\beta,\sigma} t_{\alpha\beta}(\Delta x,\Delta y)c^\dagger_{i,\alpha\sigma}c_{i+\Delta x+\Delta y,\beta\sigma}|\Delta x|^2,$$
$$\hat{T}_y = \sum_{i,\Delta x,\Delta y,\alpha,\beta,\sigma} t_{\alpha\beta}(\Delta x,\Delta y)c^\dagger_{i,\alpha\sigma}c_{i+\Delta x+\Delta y,\beta\sigma}|\Delta y|^2, \tag{7}$$

and the current operators are given by

$$\hat{J}_x = i\sum_{i,\Delta x,\Delta y,\alpha,\beta,\sigma} t_{\alpha\beta}(\Delta x,\Delta y)c^\dagger_{i,\alpha\sigma}c_{i+\Delta x+\Delta y,\beta\sigma}\Delta x,$$
$$\hat{J}_y = i\sum_{i,\Delta x,\Delta y,\alpha,\beta,\sigma} t_{\alpha\beta}(\Delta x,\Delta y)c^\dagger_{i,\alpha\sigma}c_{i+\Delta x+\Delta y,\beta\sigma}\Delta y. \tag{8}$$

One can see that both T and the current operators are closely related to the hopping integrals and hopping processes of electrons. Anisotropic kinetic energy, which is obtained from the kinetic (hopping) terms in the Hamiltonian H_0, suggests that the expected values of the x and y components of both T and the current operators in the nematic phase are expected to be unequal, resulting in anisotropic optical and dc conductivities. A more direct correlation between optical conductivity and kinetic energy is manifested by the sum rule of the optical conductivity [48], i.e., $\int_0^\infty d\omega\sigma^R_{x/y}(\omega) = -\pi\langle T_{x/y}\rangle/2$, with $\sigma^R_{x/y}$ representing the real part of the optical conductivity along the x/y direction.

Based on the above analysis, the decrease of anisotropic kinetic energy and orbital occupation as a function of electron doping density, combined with the ARPES experiment [12]

and optical spectrum measurement [36], demonstrates that the magnitude of intrinsic anisotropy is reduced upon electron doping. From this point of view, the anisotropy of dc resistivity, which becomes more pronounced with increasing Co doping [36–39], cannot be understood alone by the intrinsic electronic anisotropy. We suggest that a combination of the intrinsic nematicity with the anisotropic impurity scattering introduced by dopant Co might provide a comprehensive understanding of the dc anisotropy in FeSCs.

IV. CONCLUSIONS

In conclusion, we have demonstrated that the nematic state in FeSCs can be driven by electron correlations. Our results emphasize that the off-site Coulomb interaction V between NN Fe ions plays an important role. We obtain the condensation energy E_{cond} and the optimized order parameter $\delta_{\mathrm{var}}^{\mathrm{opt}}$ in the nematic state as functions of doping, and show that the suppression of $\delta_{\mathrm{var}}^{\mathrm{opt}}$ upon electron doping is consistent with the intrinsic anisotropies observed by optical spectrum measurement and ARPES experiments. We propose that the combination of intrinsic nematicity with anisotropic impurity scattering might provide a comprehensive understanding of the dc anisotropy in FeSCs.

ACKNOWLEDGMENTS

This work was supported by the NSFC of China under Grants No. 11074257 and No. 11274310. Z.B.H. was supported by NSFC under Grants No. 11174072 and No. 91221103, and by Specialized Research Fund for the Doctoral Program of Higher Education under Grant No. 20104208110001. Numerical calculations were performed in Center for Computational Science of CASHIPS.

[1] S. A. Kivelson, E. Fradkin, and V. J. Emery, Nature (London) **393**, 550 (1998).
[2] E. Fradkin, S. A. Kivelson, M. J. Lawler, J. P. Eisenstein, and A. P. Mackenzie, Annu. Rev. Condens. Matter Phys. **1**, 153 (2010).
[3] R. A. Borzi, S. A. Grigera, J. Farrell, R. S. Perry, S. J. S. Lister, S. L. Lee, D. A. Tennant, Y. Maeno, and A. P. Mackenzie, Science **315**, 214 (2007).
[4] V. Hinkov, D. Haug, B. Fauqué, P. Bourges, Y. Sidis, A. Ivanov, C. Bernhard, C. T. Lin, and B. Keimer, Science **319**, 597 (2008).
[5] R. Daou, J. Chang, D. Leboeuf, O. Cyr-Choinière, F. Laliberté, N. Doiron-Leyraud, B. J. Ramshaw, R. Liang, D. A. Bonn, W. N. Hardy, and L. Taillefer, Nature (London) **463**, 519 (2010).
[6] M. J. Lawler, K. Fujita, J. Lee, A. R. Schmidt, Y. Kohsaka, C. K. Kim, H. Eisaki, S. Uchida, J. C. Davis, J. P. Sethna, and E.-A. Kim, Nature (London) **466**, 347 (2010).
[7] M. H. Fischer and E.-A. Kim, Phys. Rev. B **84**, 144502 (2011).
[8] B. Edegger, V. N. Muthukumar, and C. Gros, Phys. Rev. B **74**, 165109 (2006).
[9] K. Sun, M. J. Lawler, and E.-A. Kim, Phys. Rev. Lett. **104**, 106405 (2010).
[10] X.-J. Zheng, Z.-B. Huang, and L.-J. Zou, J. Phys. Soc. Jpn. **83**, 024705 (2014).
[11] J.-H. Chu, J. G. Analytis, K. De Greve, P. L. McMahon, Z. Islam, Y. Yamamoto, and I. R. Fisher, Science **329**, 824 (2010).
[12] M. Yi, D. Lu, J.-H. Chu, J. G. Analytis, A. P. Sorini, A. F. Kemper, B. Moritz, S.-K. Mo, R. G. Moore, M. Hashimoto, W.-S. Lee, Z. Hussain, T. P. Devereaux, I. R. Fisher, and Z.-X. Shen, Proc. Natl. Acad. Sci. USA **108**, 6878 (2011).
[13] S. Kasahara, H. J. Shi, K. Hashimoto, S. Tonegawa, Y. Mizukami, T. Shibauchi, K. Sugimoto, T. Fukuda, T. Terashima, A. H. Nevidomskyy, and Y. Matsuda, Nature (London) **486**, 382 (2012).
[14] C.-C. Lee, W.-G. Yin, and W. Ku, Phys. Rev. Lett. **103**, 267001 (2009).
[15] R. M. Fernandes, E. Abrahams, and J. Schmalian, Phys. Rev. Lett. **107**, 217002 (2011).
[16] R. M. Fernandes, A. V. Chubukov, J. Knolle, I. Eremin, and J. Schmalian, Phys. Rev. B **85**, 024534 (2012).
[17] R. M. Fernandes, A. V. Chubukov, and J. Schmalian, Nat. Phys. **10**, 97 (2014).
[18] K. Nakayama, Y. Miyata, G. N. Phan, T. Sato, Y. Tanabe, T. Urata, K. Tanigaki, and T. Takahashi, Phys. Rev. Lett. **113**, 237001 (2014).
[19] Q. Deng, J. Liu, J. Xing, H. Yang, and H.-H. Wen, Phys. Rev. B **91**, 020508(R) (2015).
[20] M. D. Watson, T. K. Kim, A. A. Haghighirad, N. R. Davies, A. McCollam, A. Narayanan, S. F. Blake, Y. L. Chen, S. Ghannadzadeh, A. J. Schofield, M. Hoesch, C. Meingast, T. Wolf, and A. I. Coldea, Phys. Rev. B **91**, 155106 (2015).
[21] I. Pomeranchuk, Sov. Phys. JETP **35**, 524 (1958).
[22] C. J. Halboth and W. Metzner, Phys. Rev. Lett. **85**, 5162 (2000).
[23] B. Valenzuela and M. A. H. Vozmediano, Phys. Rev. B **63**, 153103 (2001).
[24] H. Yamase, V. Oganesyan, and W. Metzner, Phys. Rev. B **72**, 035114 (2005).
[25] C. Husemann and W. Metzner, Phys. Rev. B **86**, 085113 (2012).
[26] S. A. Kivelson, I. P. Bindloss, E. Fradkin, V. Oganesyan, J. M. Tranquada, A. Kapitulnik, and C. Howald, Rev. Mod. Phys. **75**, 1201 (2003).
[27] C. de la Cruz, Q. Huang, J. W. Lynn, J. Li, W. Ratcliff II, J. L. Zarestky, H. A. Mook, G. F. Chen, J. L. Luo, N. L. Wang, and P. Dai, Nature (London) **453**, 899 (2008).
[28] Q. Huang, Y. Qiu, W. Bao, M. A. Green, J. W. Lynn, Y. C. Gasparovic, T. Wu, G. Wu, and X. H. Chen, Phys. Rev. Lett. **101**, 257003 (2008).
[29] T. Yildirim, Phys. Rev. Lett. **101**, 057010 (2008).
[30] D. C. Johnston, Adv. Phys. **59**, 803 (2010).
[31] A. Dusza, A. Lucarelli, F. Pfuner, J.-H. Chu, I. R. Fisher, and L. Degiorgi, Europhys. Lett. **93**, 37002 (2011).
[32] M. Nakajima, T. Liang, S. Ishida, Y. Tomioka, K. Kihou, C. H. Lee, A. Iyo, H. Eisaki, T. Kakeshita, T. Ito, and S. Uchida, Proc. Natl. Acad. Sci. USA **108**, 12238 (2011).

[33] C. Fang, H. Yao, W.-F. Tsai, J. P. Hu, and S. A. Kivelson, Phys. Rev. B **77**, 224509 (2008).
[34] C.-C. Chen, J. Maciejko, A. P. Sorini, B. Moritz, R. R. P. Singh, and T. P. Devereaux, Phys. Rev. B **82**, 100504 (2010).
[35] W.-C. Lee and P. W. Phillips, Phys. Rev. B **86**, 245113 (2012).
[36] M. Nakajima, S. Ishida, Y. Tomioka, K. Kihou, C. H. Lee, A. Iyo, T. Ito, T. Kakeshita, H. Eisaki, and S. Uchida, Phys. Rev. Lett. **109**, 217003 (2012).
[37] Y. Inoue, Y. Yamakawa, and H. Kontani, Phys. Rev. B **85**, 224506 (2012).
[38] M. P. Allan, T.-M. Chuang, F. Massee, Y. Xie, N. Ni, S. L. Bud'ko, G. S. Boebinger, Q. Wang, D. S. Dessau, P. C. Canfield, M. S. Golden, and J. C. Davis, Nat. Phys. **9**, 220 (2013).
[39] S. Ishida, M. Nakajima, T. Liang, K. Kihou, C. H. Lee, A. Iyo, H. Eisaki, T. Kakeshita, Y. Tomioka, T. Ito, and S. Uchida, Phys. Rev. Lett. **110**, 207001 (2013).
[40] C. M. Puetter, J. G. Rau, and H.-Y. Kee, Phys. Rev. B **81**, 081105 (2010).
[41] S. Zhou and Z. Wang, Phys. Rev. Lett. **105**, 096401 (2010).
[42] T. Miyake, K. Nakamura, R. Arita, and M. Imada, J. Phys. Soc. Jpn. **79**, 044705 (2010).
[43] D. Ceperley, G. V. Chester, and M. H. Kalos, Phys. Rev. B **16**, 3081 (1977).
[44] C. J. Umrigar, K. G. Wilson, and J. W. Wilkins, Phys. Rev. Lett. **60**, 1719 (1988).
[45] Y. Zhang, M. Yi, Z.-K. Liu, W. Li, J. J. Lee, R. G. Moore, M. Hashimoto, N. Masamichi, H. Eisaki, S.-K. Mo, Z. Hussain, T. P. Devereaux, Z.-X. Shen, and D. H. Lu, arXiv:1503.01556.
[46] A. J. Millis and S. N. Coppersmith, Phys. Rev. B **42**, 10807 (1990).
[47] E. Dagotto, Rev. Mod. Phys. **66**, 763 (1994).
[48] W. Kohn, Phys. Rev. **133**, A171 (1964).